Enhanced mobile hybridization of gold nanoparticles decorated with oligonucleotide in microchannel devices

Miao-Hsing Hsu,[a] Wei-Feng Fang,[a] Yu-Hsuan Lai,[a] Jing-Tang Yang,*[a] Tsung-Lin Tsai[b] and Dar-Bin Shieh[b]

Received 29th March 2010, Accepted 15th June 2010
DOI: 10.1039/c004753h

Mobile hybridization is a concept proposed and verified herein. We have designed a microfluidic device that is capable of enhancing passive mixing through the morphology of micro-structures, positioned along the channels of the device. We investigated the capability of these structures to promote mobile hybridization of fluorophore-labeled target oligonucleotides to oligonucleotide gold-nanoparticle (Au-NP) probes. This process is monitored with fluorescence through the quenching of the fluorescent signal within the device as the target oligonucleotides become bound to the Au-NP probes. We evaluated the fluorescent intensity of a sample image that showed enhanced probability of mobile hybridization of the samples, which was completed in about 7.2 s. Mobile hybridization is thus much more effective than traditional static hybridization (reaction overnight) limited by molecular diffusion. This approach promises an improved hybridization of samples with these probes, and is beneficial for microfluidic-based systems for biomedical detection.

1. Introduction

Gold nanoparticles are applied in biomedical applications because of their biocompatibility, well established synthesis and surface-conjugation chemistry, and their unique optoelectronic properties. Such gold nanoparticles, modified to serve as probes or carriers to catch and to sense target molecules or organisms, have been widely used in rapid diagnosis of DNA or pathogens,[1] for highly sensitive detection of proteins[2] and for improved PCR detection.[3]

Microfluidic systems with integrated modified gold nanoparticles have been implemented for detection in real time.[4] The mixing of modified gold nanoparticles and their binding to the target objects in microchannels that determine the sensitivity and accuracy of the measurements and data interpretation have attracted little research attention. A microfluid in a laminar state typically lacks a turbulent fluctuation to accelerate flow mixing. Various active or passive devices in the mixer or reaction chamber were therefore designed to remedy the deficiency in an expectation that complete fluid mixing and reaction are achievable within such a small distance and duration.[5,6] In our preceding work,[7–10] we created various passive devices for fluidic mixing and reaction based on the principles of splitting and recombination (SAR) and of chaotic advection.

In the present project we designed an efficient microreactor based on preceding work,[10] and we propose mobile hybridization as a concept. We investigated the mobile hybridization of an oligonucleotide (target DNA) and modified gold nanoparticles (Au-NP probes) in that device. Utilizing fluorescence quenching to measure the extent of mobile hybridization, we applied a test DNA as a control to assess the mixing. The hybridization and mixing were simultaneously monitored and analyzed according to this experimental strategy. The results manifest a significant advantage of mobile hybridization over traditional static hybridization in greatly decreasing the duration of reaction.

2. Concept

The objective of the experiment was to analyze the hybridization of a target DNA and modified gold nanoparticles in microchannels as shown in Fig. 1. The modified gold nanoparticles (Au-NP probes) flow from one end of the flow channel, one entry; the target and test DNA flow from the other entry. Synthesis of the Au-NP probe results from modifying the surface of gold nanoparticles (Au-NP, 13-nm) with a single-strand DNA (sequence: 5′–SH-TTTTTTTTTTTTTTTTTTT–3′). The fluorochrome FAM was conjugated on the target DNA (5′–FAM-AAAAAAAAAAAAAAAAAAA–3′). The test DNA was modified with fluorochrome TAMRA (5′–TAMRA-CCCCCCCCCCCCCCCCCCC–3′).

Fig. 1 shows that, at the confluence of the microchannels, target DNA and control DNA have not mixed and bound to the Au-NP probe because the emission spectra clearly contain two separate signals from the fluorescence of each of FAM and TAMRA. After passing through the reaction channel, the target DNA binds to the Au-NP probe causing a significant quenching of the FAM fluorescence by the gold nanoparticles (Au-NP absorb light about 520 nm). Through monitoring the two fluorescent spectral signals, we follow the extent of hybridization between the target DNA and the Au-NP probes, and thus observe the dispersion of the test DNA without hybridization in the microchannels. Using this experimental design, we simultaneously analyzed the hybridization and the mixing of the DNA and nanoparticle probes in the microchannels.

[a]*Department of Mechanical Engineering, National Taiwan University, Taipei, 10617, Taiwan. E-mail: jtyang@ntu.edu.tw; Fax: 886-(2)-3366-9548; Tel: 886-(2)-3366-9875*
[b]*Institute of Oral Medicine, College of Medicine, National Cheng Kung University, Tainan, 70101, Taiwan*

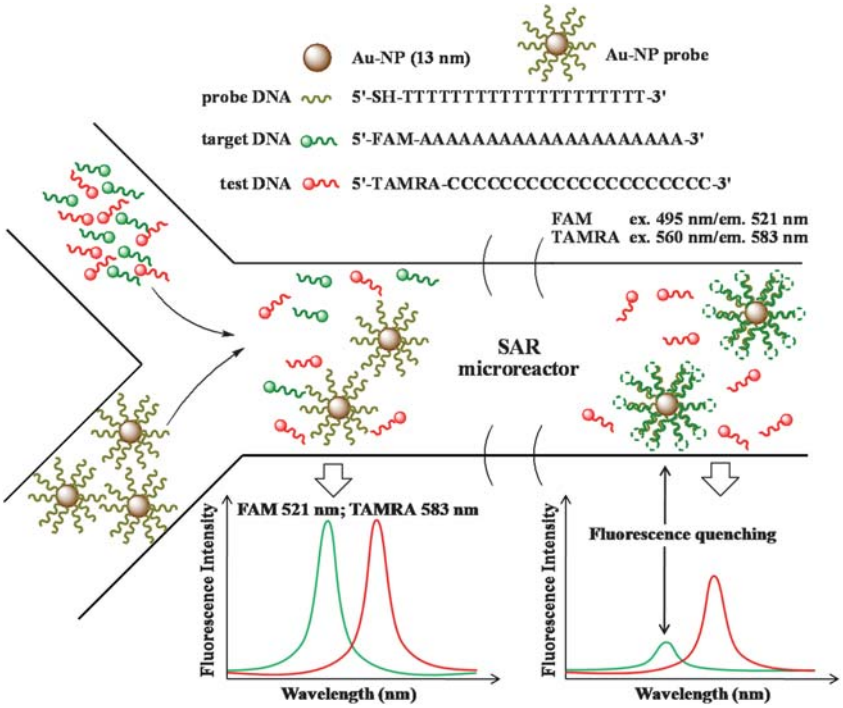

Fig. 1 Analytic strategy for mobile hybridization.

3. Experiments

The Y-shaped microchannel and SAR micro-reactor were made of polydimethylsiloxane (PDMS), which is highly biocompatible and readily manufactured. Using a standard photolithographic technique, we made a master mold for the reactor on a silicon substrate with a negative photoresist (SU-8, MicroChem Corporation 2035). The prepared mixtures of PDMS and a curing agent were poured onto the SU-8 mold. After curing at 80 °C for 2 h in an oven, the PDMS solidified as a plate complementary to the mold and was then peeled from the mold. After the PDMS layer and a cover slide were activated with an oxygen plasma, the Y-shaped microchannel was packaged. As the upper and lower plates of the SAR micro-reactor have identical patterns, the replicate process with the same mold was simple. To bind these two plates of the microreactor, the surfaces of PDMS were activated with an oxygen plasma, with methanol as a surfactant to lubricate the binding interface that enabled the alignment of the plates with custom instruments. The Y-shaped microchannel has a total length 106 mm; the depth of the channel is about 50 μm, as shown explicitly in Fig. 2a. Compared with other reported micro-mixing devices with intricate microstructures in the channels that require complicated fabrication to achieve improved mixing performance,[11–13] the master mold of our SAR micro-reactor from photolithography provides a simple, one-step fabrication of the system. The SAR micro-reactor is shown in Fig. 2b, which also presents SEM photographs of the top view, an oblique drawing and a magnified image with detailed dimensions of the microchannel. The angle of the dividing edge is 53°, and the depth of the channel is about 50 μm, as shown in the lower right image of Fig. 2b.

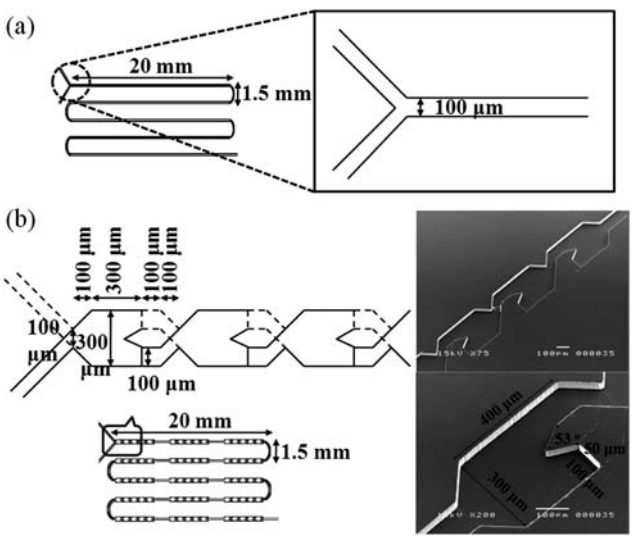

Fig. 2 (a) Schematic illustration of the straight geometry; (b) SAR microreactor geometry and configuration. Images on the right hand side are SEM photos of the channel with detailed dimensions.

One inflow contained fluorophore solutions with a 20-mer adenine sequence of oligonucleotide modified with 5′–FAM (6-carboxyfluorescein, $\lambda_{ex} = 495$, $\lambda_{em} = 521$ nm, target DNA) (1×10^{-6} M, MDBio Inc., Taiwan) and a 20-mer cytosine sequence of oligonucleotide modified with 5′–TAMRA ($\lambda_{ex} = 560$, $\lambda_{em} = 583$ nm, test DNA) (1×10^{-6} M, MDBio Inc., Taiwan). The other inflow was a buffer solution (phosphate-buffered saline, PBS, pH = 7.4) containing a 20-mer thymine sequence of oligonucleotide modified with Au-NP (13 nm, 1×10^{-8} M, prepared as previously described).[14] The average oligonucleotide surface coverage of

alkanethiol-modified 20-mer oligonucleotide on Au nanoparticles was 30 pmol cm^{-2}. For 13-nm Au-NP, this condition corresponds to roughly 100 thiol-bound 20-mer strands per gold particle. All experiments were conducted with the flow driven with pressure generated by a syringe pump (KDS220 syringe pump, KD Scientific Inc.). The flow rate was controlled through the setting of the syringe pump (3 mm s^{-1}).

The mixing patterns of fluids in the devices were visualized with a confocal microscope (Nikon A1R). All optical measurements were performed at 25 °C under ambient conditions; a schema of the light path appears in Fig. 3. The excitation light, provided with a diode laser (488 nm) and argon laser (561 nm), was directed into resonant mirrors in a set to produce rapid line scanning. The laser beams were then directed into an objective lens (plane apochromat VC 10×, NA = 0.45) with a dichroic mirror, which reflects light at wavelengths 405, 488 and 561 nm and transmits other wavelengths. The sampled volume was uniformly illuminated line by line with laser beams; emission therefrom was collected with the same objective lens. To eliminate stray light, the emitted light was directed to pass a pinhole (diameter 12.8 μm) behind the dichroic mirror. The intensities of the light emitted in wavelength range 500–600 nm, selected with filters, were measured with two separate photomultiplier tubes (PMT).

4. Results and discussion

4.1 Calibration curves

To establish a calibration curve, one seeks a linear relation over a sufficient analytical range between the concentration of fluorescer and the fluorescent intensity; on this basis one sets the operating conditions of a confocal microscope (laser intensity, detection gain, size of pinhole *etc.*) to intercept the fluorescence over a varied DNA concentration (10^{-6}–10^{-7} M) in the flow channel. Fig. 4 shows calibration curves of FAM and TAMRA fluorescence and a relation between fluorescence intensity and concentration, for a concentration range 10^{-6}–10^{-7} M that is satisfactory for analysis under fixed operating conditions; the concentration of fluorescer is deduced on measuring the intensity of fluorescence of the solution.

4.2 Reaction of the samples in microchannels

The solution containing FAM-tagged target DNA and test DNA with TAMRA flows through one entry of the channel and the Au-NP probe flows through the other entry. We compared the effect of mixing and reaction of samples in a straight channel having no structure with those in the reaction channel proposed in this work.

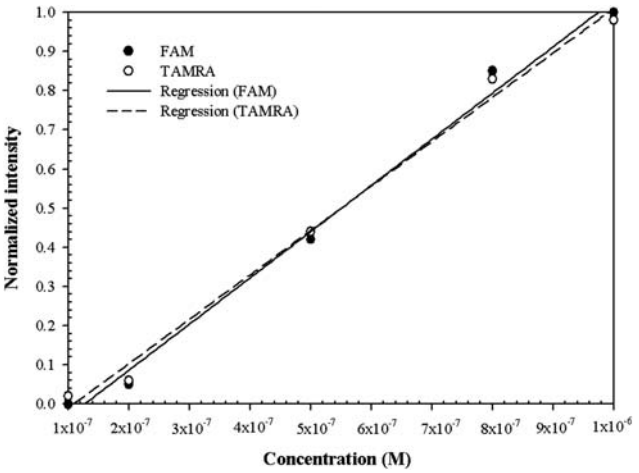

Fig. 4 Calibration curves for fluorescence of FAM and TAMRA.

The behavior of test DNA in a straight channel, as shown in images 1 to 22 in Fig. 5, reveals that the fluid mixes slowly as the primary driving force of the fluid mixture in such a channel, based mainly on diffusion between molecules, is generally inefficient. Concurrently with the test DNA gradually diffusing and mixing from upstream to downstream, the concentration of fluorescer decreases through dilution, and the fluorescent intensity correspondingly diminishes. For the target DNA, the results indicate that the reaction is similar to the mixing of test DNA; only little target DNA hence hybridized to the Au-NP probe, and the fluorescent intensity decreased only slightly, similarly to diffusive mixing.

For the newly designed reaction channel, the mixing of test DNA in the flow channel differs from that of the straight channel in that the structural design significantly promoted the rapid mixing of the test DNA so that a uniform state at every stage (images 6–22, as shown in Fig. 6) was already achieved. For the target DNA, every image showed satisfactory uniformity, but the intensity of the image gradually decreased (darkened) from upstream to downstream. In addition to the mixing between fluids in the process, the intensity of target DNA fluorescence

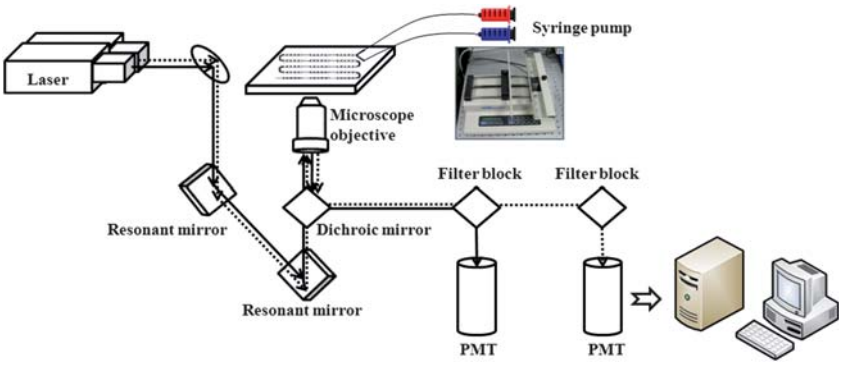

Fig. 3 Schematic diagram of the experimental apparatus.

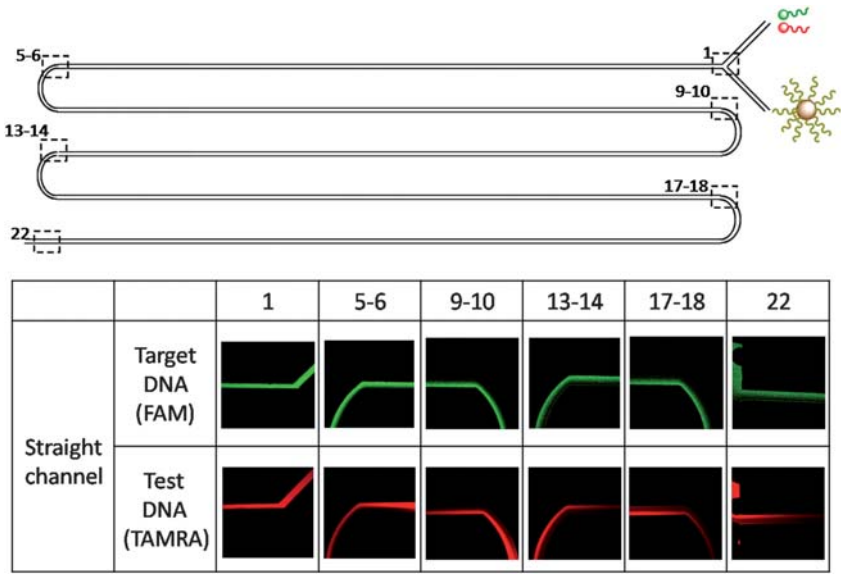

Fig. 5 Scheme for hybridization of the Au-NP probe, target DNA, and test DNA in the straight microchannel.

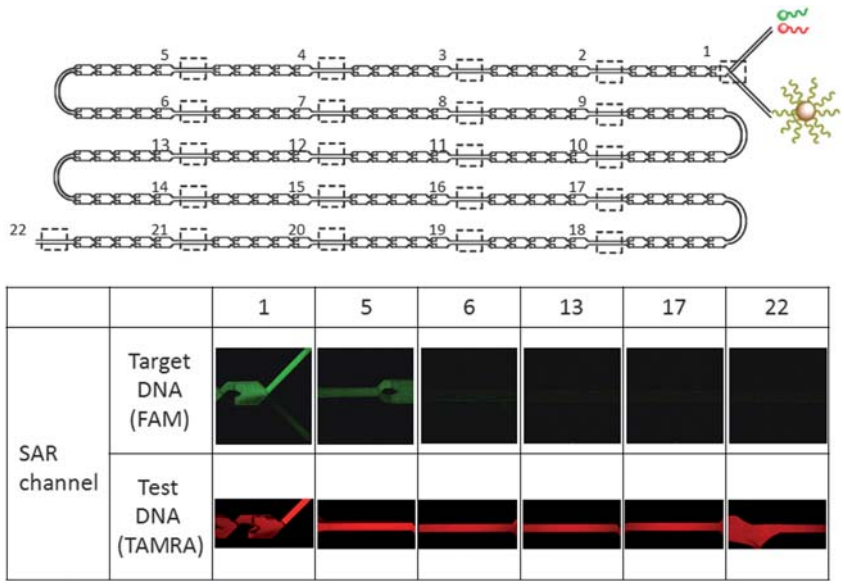

Fig. 6 Scheme for hybridization of the Au-NP probe, target DNA, and test DNA in the SAR microreactor.

decreased because of quenching by Au-NP upon hybridization of target DNA to the probes.

4.3 Quantification of mixture and reaction

To quantify the sample reaction and mixing distance in a flow channel, we analyzed the captured images with 12-bit gray-level intensity. With data processing of the sampled images, we calculated the average intensity of all pixels. The normalized intensity (I') is defined as

$$I' = \frac{\bar{I} - I_{\min}}{I_{\max} - I_{\min}} \quad (1)$$

in which $I_{\max}$ and $I_{\min}$ are the maximum and minimum intensities, respectively, of pixels from all sampled images; $\bar{I}$ is the average intensity of a sampled image. As all curves converge to a common value downstream, the region downstream from the hybridization or mixing reaction is stable. The continuous flow presents a dynamic equilibrium, and the completion of the hyridization and the mixing is adjustable with the convergence value (minimum value) of the curve. The required distance and duration of the reaction and mixture thus become defined.

For the test DNA, the mixture in a straight channel is dominated by diffusion; with mixing length L, average speed U of flow, diffusion length d, diffusion coefficient D, Péclet number Pe, the relation is[15]

$$L \sim U \times \frac{d^2}{D} = \mathrm{Pe} \times d \quad (2)$$

The length required for homogenous mixing is thus calculated to be about 30 mm when the flow rate is 3 mm s^{-1} and the diffusion coefficient of DNA is 10^{-10} m^2 s^{-1}. From the mixing curve of test DNA in a straight channel, a state near complete mixing required about 90 mm, longer than predicted because of the disparate densities of the two fluids. Although the centrifugal force results in a transverse mass transfer and accelerates the fluid mixing, this action does not make target DNA conjugate properly with the Au-NP probe. The hybridization curve of the target DNA is similar to that of the mixing reaction.

For the newly designed reaction channel, the test DNA attained complete mixing rapidly and presented a homogenous distribution of fluorescent intensity in images 6 to 22. The fluid hence achieved completely homogenous mixing before the first corner (about 21.8 mm). As deduced from the curve in Fig. 7, the mixing distance of the fluid in the reaction channel is less than 21.8 mm. For the target DNA, the effect of the structure of the flow channel makes DNA not only mix rapidly with the other flow, but also accelerates and enhances the efficiency of hybridization. When target DNA moves from upstream to downstream, the fluorescent intensity is similar to that of the complete mixing at the first corner. The fluorescence tends to become quenched further downstream, indicating that the target DNA reacts rapidly and continuously with the Au-NP probes. The fluorescent intensity in a steady state implies that the hybridization of the target DNA and the Au-NP probe has attained saturation. The duration of hybridization is about 7.2 s from the estimated period of retention. For the hybridization to be completed in the straight channel takes 15 min. According to the traditional static hybridization, the hybridization occurs through diffusion of the driving fluid; an overnight period is typically required to improve the hybridization. According to the concept of our microfluidic system, mobile hybridization occurs between samples, thus enhancing the speed and efficiency of hybridization by means of the channel microstructure design.

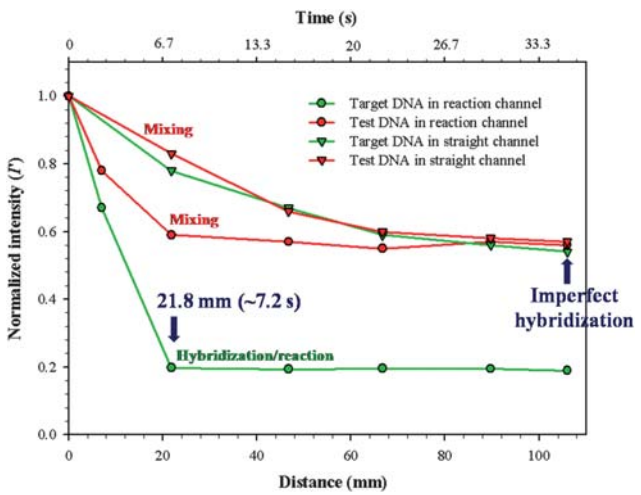

Fig. 7 Normalized intensity and duration of reaction for hybridization of the Au-NP probe, target DNA and test DNA in the straight and SAR microreactors.

5. Conclusion

We have demonstrated the concept mobile hybridization by verifying the conjugation of DNA with modified gold nanoparticles in a designed microreactor. In the hybridization experiment, the samples and probes flow through Y-shaped channels simultaneously for a dynamic mobile hybridization in the microreactor. The effect of the structure in the microreactor enables the reaction to attain saturation in only 7.2 s, a duration much less than for traditional static hybridization. In medical tests, one can diagnose the result in a flow channel in real time. In our experiment, the mixing and hybridization of target and test DNA with the Au-NP probes are monitored concurrently in the microreactor. The results show that the microreactor presents a length of travel to achieve complete hybridization near the length required for only homogenous mixing, but the required duration is much smaller than that required for traditional static hybridization systems that typically require a few hours. The practice of mobile hybridization in a sample is significantly improved through the structural design of the microreactor presented here.

Acknowledgements

National Science Council of the Republic of China partially supported this work under contract NSC 96-2628-E-002-257-MY3 and NSC 98-2218-E-002-024.

References

1 T. A. Taton, C. A. Mirkin and R. L. Letsinger, *Science*, 2000, **289**, 1757.
2 C. C. You, O. R. Miranda, B. Gider, P. S. Ghosh, I. B. Kim, B. Erdogan, S. A. Krovi, U. H. Bunz and V. M. Rotello, *Nat. Nanotechnol.*, 2007, **2**, 318.
3 J. M. Nam, S. I. Stoeva and C. A. Mirkin, *J. Am. Chem. Soc.*, 2004, **126**, 5932.
4 E. D. Goluch, J. M. Nam, D. G. Georganopoulou, T. N. Chiesl, K. A. Shaikh, K. S. Ryu, A. E. Barron, C. A. Mirkin and C. Liu, *Lab Chip*, 2006, **6**, 1293.
5 N. T. Nguyen and Z. Wu, *J. Micromech. Microeng.*, 2005, **15**, R1–R16.
6 V. Hessel, H. Löwe and F. Schönfeld, *Chem. Eng. Sci.*, 2005, **60**, 2479.
7 J. T. Yang, K. J. Huang and Y. C. Lin, *Lab Chip*, 2005, **5**, 1140.
8 J. T. Yang, K. J. Huang, K. Y. Tung, I. C. Hu and P. C. Lyu, *J. Micromech. Microeng.*, 2007, **17**, 2084.
9 J. T. Yang, W. F. Fang and K. Y. Tung, *Chem. Eng. Sci.*, 2008, **63**, 1871.
10 W. F. Fang and J. T. Yang, *Sens. Actuators, B*, 2009, **140**, 629.
11 J. Cha, J. Kim, S. K. Ryu, J. Park, Y. Jeong, S. Park, S. Park, H. C. Kim and K. Chun, *J. Micromech. Microeng.*, 2006, **16**, 1778.
12 S. W. Lee and S. S. Lee, *Sens. Actuators, B*, 2008, **129**, 364.
13 T. Tofteberg, M. Skolimowski, E. Andreassen and O. Geschke, *Microfluid. Nanofluid.*, 2010, **8**, 209.
14 A. D. McFarland, C. L. Haynes, C. A. Mirkin, R. P. Van Duyne and H. A. Godwin, *J. Chem. Educ.*, 2004, **81**, 544A.
15 A. D. Stroock, S. K. Dertinger, A. Ajdari, I. Mezic, H. A. Stone and G. M. Whitesides, *Science*, 2002, **295**, 647.